

# Line and Planar Defects with Zero Formation Free Energy: Applications of the Phase Rule toward Ripening-Immune Microstructures

Ju Li<sup>1,2</sup> and Yuri Mishin<sup>3</sup>

<sup>1</sup> Department of Nuclear Science and Engineering, Massachusetts Institute of Technology, Cambridge, MA 02139, USA

<sup>2</sup> Department of Materials Science and Engineering, Massachusetts Institute of Technology, Cambridge, MA 02139, USA

<sup>3</sup> Department of Physics and Astronomy, MSN 3F3, George Mason University, Fairfax, Virginia 22030, USA

## Abstract

Extended one- and two-dimensional defects in crystalline materials are usually metastable. The thermodynamic ground state of the material is presumed to be defect-free. Here, we investigate the conditions under which extended defects, such as grain boundaries, can exist in a multicomponent alloy when the latter reaches the thermodynamic ground state allowed by the Gibbs phase rule. We treat all extended defects as low-dimensional phases on the same footing as the conventional bulk phases. Thermodynamic analysis shows that, in the ground state, the formation free energies of all extended defects must be zero, and the system must follow a generalized phase rule. The latter predicts that only a finite number of symmetry-related defect types can coexist in the material in the ground state. Guided by the phase rule, we discuss finite-size polycrystalline and/or polyphase microstructures that are fully immune to coarsening and their possible transformations.

# 1 Introduction

Most crystalline solids contain defects, which are traditionally classified into the following categories:

- Zero-dimensional (0D) defects, also known as point defects, include vacancies, self-interstitials, impurity atoms, and similar disruptions of crystalline order with atomic-scale size in all directions.
- One-dimensional (1D) defects, including dislocations, triple junctions of grains in polycrystalline materials, contact lines between phases, and other defects with atomic-scale dimensions in two directions and mesoscale length along a line.
- Two-dimensional (2D) defects, such as grain boundaries, interphase boundaries, stacking faults, and other defects of mesoscale area and atomic-scale width.

3D defects can also be considered, such as pores and stacking-fault tetrahedra, but they are not discussed in this paper. The 1D and 2D defects are collectively referred to as extended defects.

Intrinsic point defects, such as vacancies and self-interstitials, are classified as *equilibrium defects* because they are part of the thermodynamic ground-state structure of crystalline phases. At a given temperature  $T$ , they reach equilibrium concentrations

$$c^{\text{eq}}(T) \propto \exp(-f_{0\text{D}}/k_{\text{B}}T), \quad (1)$$

where  $f_{0\text{D}}$  is the local (non-configurational) formation free energy per defect and  $k_{\text{B}}$  is Boltzmann's constant. The intrinsic point defects form spontaneously to reduce the Helmholtz free energy of the solid by increasing its configurational entropy. The latter is associated with different positions of the defects on the crystalline lattice, which they sample by a diffusive random walk.

In contrast, most extended defects are thermodynamically unstable or metastable. They have an excess non-configurational free energy, and seldom contribute to the configurational entropy because their mobility is too low, preventing them from sampling the positions in space on the timescale of laboratory experiments and practical applications. As a result, their formation free energy is dominated by the non-configurational part. Its value per unit length  $L$  or per unit area  $A$  is often referred to as, respectively, the free energy of the line  $\tau$  and the free energy of the surface/interface  $\gamma$ . These quantities are sometimes called line tension and surface tension, respectively, if directional isotropy is assumed (e.g., fluid/fluid interfaces). An extended defect cannot form spontaneously by thermal fluctuations because

its total formation free energy is exorbitantly high. For example, the total free energy  $F = \tau L$  of a dislocation line of length  $L$  (typically measured in micrometers) can be on the order of keV or higher. As a result, the thermally equilibrium population of dislocations, estimated from the Boltzmann factor  $\propto \exp(-F/k_B T)$ , is negligibly small. The same applies to the thermally equilibrium population of grain boundaries.

Extended defects can lower their length/area spontaneously if they possess sufficient mobility. They can also increase their length/area if an external driving force is applied, such as shear stress, radiation, or temperature change. For example, a Peach-Koehler force acting on a dislocation can cause it to bow out and increase its length. In many cases, extended defects are found in a stationary state when they are pinned by immobile elements of the microstructure. Stationary defects can reach a state of *constrained* thermodynamic equilibrium, i.e., equilibrium with respect to exchanges of heat and chemical components with the environment. In alloy systems, such exchanges lead to the formation of solute segregation at interfaces and segregation atmospheres (Cottrell atmospheres) at dislocations. The solute segregation reduces the free energy of defect formation according to the Gibbs adsorption equation for multicomponent systems [1], but the latter remains positive in most cases. We emphasize that the defect is *not* in full thermodynamic equilibrium because its length/area is not allowed to vary to further reduce the free energy.

It was suggested [2–20] that a sufficiently strong grain boundary segregation of solute atoms can fully stabilize a polycrystalline alloy against grain growth. Thermodynamic analysis shows that the total free energy of a closed system composed of a uniform grain boundary and surrounding grains can reach a minimum with respect to variations of the boundary area when the boundary free energy  $\gamma$  reaches zero value [19]. The derivation assumes that during the area variations, the grain boundary remains in thermal and chemical equilibrium with the grains. Extensive experimental, theoretical, and computational efforts [10–26] have been dedicated to the search for solutes that could drastically reduce  $\gamma$  and even drive it to a zero value. However, the thermodynamic meaning of the conditions of  $\gamma = 0$  or  $\tau = 0$  and their microstructural consequences have not been systematically discussed.

Here, we suggest that the thermodynamics underlying the grain boundary stabilization is as general as the thermodynamics of 3D phases, in which multiple 3D phases can coexist in equilibrium if certain thermodynamic conditions are met. Thermodynamics is equally valid for all 2D and all 1D defect phases in crystalline materials. For 1D defects, the  $\gamma = 0$  condition must be replaced with  $\tau = 0$ . A truly stabilized material must satisfy the  $\gamma = 0$  and  $\tau = 0$  conditions for *all* 2D and 1D defects present in the material. For example, if all grain boundaries in a polycrystalline material are fully stabilized ( $\gamma = 0$ ) but  $\tau$  of triple

junctions remains positive, the defect structure will still remain unstable and evolve under the capillary forces of the triple junctions. The total free energy will continue to strive towards smaller values.

The full thermodynamic stabilization of crystalline materials is an important fundamental concept, but it also presents significant practical interest. The pursuit of full thermodynamic stabilization of polycrystals and/or finite-size phases (e.g., phase precipitates) that are forever immune to Ostwald ripening or coarsening opens a previously unrecognized design space, particularly for nanocrystalline materials whose superior physical and mechanical properties predicate on the suppression of grain growth at elevated temperatures. The full thermodynamic stabilization, if achieved, will suppress all driving forces while retaining the nanostructure responsible for the superior properties. The full stabilization concept is very general and relies only on the laws of thermodynamics. If realized in practice, it would circumvent the currently employed kinetic stabilization mechanisms such as solute drag and Zener pinning by small embedded particles.

The central idea of this article is that extended defects can be treated as 1D and 2D phases on par with conventional bulk (3D) phases. Thus, the material can be considered to be composed of multiple phases of different dimensionality: 1D and 2D phases of extended defects and 3D bulk phases. Generally, these phases are not in equilibrium with each other. However, the system can reach the thermodynamic ground state if all phases establish equilibrium with each other. It can be shown (see Supplementary Information) that the condition of  $\gamma = 0$  and  $\tau = 0$  for all defects is equivalent to achieving the thermodynamic equilibrium between all phases present in the system. This insight is crucial because it allows us to apply the Gibbs phase rule to the fully stabilized crystalline material containing defects. Depending on the number of chemical components, the phase rule can predict the maximum numbers of different 1D and 2D defects that can coexist in the system when it reaches the ground state. These numbers inform the analysis of possible equilibrium microstructures of a fully stabilized material, depending on the dimensionalities of the defects and the crystal symmetry. Such microstructures could be designed to achieve the desired physical and mechanical properties while simultaneously preventing them from coarsening at high temperatures.

## 2 Thermodynamics of extended defects and the phase rule

We consider a  $k$ -component alloy composed of several bulk phases and grains. The alloy contains interfaces and line defects. The extended defects are treated as phases on equal

footing with the bulk phases. For brevity, we will use the shorthand  $(\varphi_3@ \varphi_2@ \varphi_1)_k$  for a  $k$ -component system composed of  $\varphi_3$  bulk phases,  $\varphi_2$  2D phases, and  $\varphi_1$  1D phases. For example,  $(1@1@0)_2$  denotes a single-phase binary solid solution containing a grain boundary.

Thermodynamic properties of a bulk phase are fully defined by a fundamental equation

$$F = F(T, N_1, \dots, N_k, V), \quad (2)$$

where  $F$  is the total free energy of the phase,  $T$  is temperature,  $V$  is volume, and  $N_i$  are the amounts of the chemical components (in moles). The phase is considered spatially uniform and thermally equilibrated (uniform temperature throughout). Under these assumptions, the free energy is a homogeneous first-degree function of  $V$  and all  $N_i$ 's. Applying Euler's theorem of homogeneous functions, we obtain

$$F = -pV + \sum_{i=1}^k \mu_i N_i, \quad (3)$$

where  $\mu_i = \partial F / \partial N_i$  are the chemical potentials of the components and  $p = -\partial F / \partial V$  is pressure.

Next, consider an interface between two phases or two grains in the same phase. All thermodynamic properties of the interface can be derived from its fundamental equation [27, 28]

$$\tilde{F} = \tilde{F}(T, \tilde{N}_1, \dots, \tilde{N}_k, A), \quad (4)$$

where  $A$  is the interface area,  $\tilde{F}$  is the excess free energy of the interface, and  $\tilde{N}_i$  are the excess amounts of the chemical components (in moles). There are many ways to define interface excess properties [27, 29], which all lead to the same final results. In Eq.(4), the excesses are defined using Gibbs' dividing surface construction [30]. Namely, the excess quantity is calculated relative to homogeneous bulk phases by extrapolating their intensive properties to the geometric dividing surface. Note that Eq.(4) has the same functional form as Eq.(2), except that the spatial dimensions of the interface are defined by its area  $A$  instead of the volume  $V$ . The interface properties are assumed to be uniform throughout the area. Therefore, the excess free energy in Eq.(4) is again a homogeneous function of first degree with respect to the extensive variables  $A$  and  $\tilde{N}_i$ 's. From Euler's theorem,

$$\tilde{F} = \gamma A + \sum_{i=1}^k \tilde{\mu}_i \tilde{N}_i. \quad (5)$$

Here,

$$\gamma = \frac{\partial \tilde{F}}{\partial A} \quad (6)$$

is the interface free energy (tension) and we introduced the notation  $\tilde{\mu}_i \equiv \partial \tilde{F} / \partial \tilde{N}_i$ . Note that  $\gamma$  is a 2D analog of the (negative) pressure  $p$ .

Similarly, all thermodynamic properties of a line defect can be derived from the fundamental equation [27, 28]

$$\hat{F} = \hat{F}(T, \hat{N}_1, \dots, \hat{N}_k, L), \quad (7)$$

where  $L$  is the defect length and the excess quantities are calculated by extrapolating the intensive properties of the homogeneous bulk phases to the defect line. The excess free energy in Eq.(7) is a homogeneous function of first degree similar to Eq.(2) except for the replacement of  $V$  by  $L$ . As above, we apply Euler's theorem to obtain

$$\hat{F} = \tau A + \sum_{i=1}^k \hat{\mu}_i \hat{N}_i, \quad (8)$$

where  $\hat{\mu}_i \equiv \partial \hat{F} / \partial \hat{N}_i$  and

$$\tau = \frac{\partial \hat{F}}{\partial L} \quad (9)$$

is the defect free energy (line tension), which is a 1D analog of the interface tension  $\gamma$ .

The similarity of the fundamental equations (2), (4) and (7) justifies treating the extended defects as phases. As indicated earlier [27], the laws of thermodynamics are not specific to any particular dimension of space. Any object whose thermodynamic properties are described by a fundamental equation can be treated as a phase. Thermodynamically, a 3D phase is no different from 1D/2D defect phases or other low-dimensional systems such as suspended graphene, graphene, or twisted MoS<sub>2</sub> bilayer.

The total free energy of a multiphase, multidefect system is the sum of the free energies of all phases present in the system in the form of equations (2), (4) and (7). Suppose that the phases are initially not in equilibrium with each other. Then we bring them to thermal, mechanical, and chemical equilibrium with each other. As discussed in the Supplementary Information file, the equilibrium conditions can be readily derived by considering reversible variations of the temperatures of all phases and volumes of the bulk phases, as well as exchanges of the chemical components between the phases. The result is that the temperatures of all phases must be equal, the pressures in the bulk phases must be equal, and the coefficients in front of  $\tilde{N}_i$  and  $\tilde{N}_i$  in Eqs.(5) and (8) must be equal to the respective chemical potentials:  $\hat{\mu}_i = \tilde{\mu}_i = \mu_i$  for all  $i = 1, \dots, k$ . In other words, the chemical potential of each species is the same in all phases of any dimensionality. Under these conditions, Eqs.(5) and (8) become

$$\tilde{F} = \gamma A + \sum_{i=1}^k \mu_i \tilde{N}_i, \quad (10)$$

$$\hat{F} = \tau L + \sum_{i=1}^k \mu_i \hat{N}_i. \quad (11)$$

The above conditions of thermal, mechanical, and chemical equilibrium are not sufficient for reaching the thermodynamic ground state. They only bring the system to a state of constrained equilibrium, in which the segregation atmospheres on extended defects are in equilibrium with the bulk phases, but the defects are not allowed to alter their areas and lengths. To reach the ground state, the free energy must be minimized with respect to variations of the defects' areas and lengths. The result of this minimization (see Supplementary Information file) is that in the ground state, the formation free energies of all extended defects must be zero:

$$\tau_1 = \tau_2 = \dots = \tau_{\varphi_1} = 0, \quad (12)$$

$$\gamma_1 = \gamma_2 = \dots = \gamma_{\varphi_2} = 0. \quad (13)$$

The possible defect configurations in the ground state will be discussed later.

The system can remain in the ground state while some of its thermodynamic parameters vary without changing the number of phases. The number  $\pi$  of independent parameters that can vary (the number of degrees of freedom) can be derived by subtracting the total number of constraints imposed by the equilibrium conditions from the total number of intensive parameters describing the system. The calculation gives the following phase rule for a crystalline material with defects (see Supplementary Information file):

$$\pi = k + 2 - (\varphi_1 + \varphi_2 + \varphi_3). \quad (14)$$

For example, consider a  $(1@1@0)_2$  system composed of a binary solid solution with a grain boundary (or a set of symmetrically equivalent grain boundaries) at  $\gamma = 0$ . Eq.(14) predicts  $\pi = 2$ . If the pressure is fixed, the system has one degree of freedom. For example, we can vary the temperature, which will cause changes in grain boundary segregation, the chemical composition of the grains, and the grain boundary area. If we also fix the temperature, then there will be no degrees of freedom left. We can still vary the average chemical composition of the alloy by adding or removing the solute atoms. This will not cause any changes in the chemical composition inside the grains or at the grain boundary. However, the grain boundary area will vary to accommodate the added/removed solute atoms. The same solid solution can be equilibrated with two different grain boundaries (assuming that they represent different 2D phases), but only at one temperature.

As another example, consider a tri-crystal (three grain boundaries and a triple line) in a five-component solid solution, which is a  $(1@3@1)_5$  system. When this system reaches a

thermodynamic ground state, it has  $\pi = 2$  degrees of freedom. At a fixed pressure, the temperature can be varied while keeping the system in the ground state. Temperature variations will be accompanied by changes in grain composition and boundary/junction segregations with corresponding adjustments of their areas/lengths.

We next discuss a geometric interpretation of the defect thermodynamics. It is convenient to reformulate the fundamental equations in intensive variables. For a bulk phase, we introduce the molar free energy  $f = F/N$  and the concentrations (mole fractions) of the components  $c_i = N_i/N$ , where  $N = \sum_i N_i$  is the total amount of the chemical components. The chemical composition is specified by  $(k - 1)$  independent concentrations, for which we choose  $c_2, \dots, c_k$ . These concentrations form a  $(k - 1)$ -dimensional composition vector  $\mathbf{C} = (c_2, \dots, c_k)$ . Eqs.(2) and (3) become

$$f = f(T, c_1, \dots, c_k, \omega), \quad (15)$$

$$f = -pV + \left( \mu_1 + \sum_{i=2}^k \mu_{i1} c_i \right), \quad (16)$$

where  $\omega = V/N$  is the molar volume and  $\mu_{i1} = \mu_i - \mu_1$  are diffusion potentials relative to the reference component 1. Similarly, for the excess free energy of an extended defect we have

$$\tilde{f} = \tilde{f}(T, \tilde{c}_1, \dots, \tilde{c}_k, \sigma), \quad (17)$$

$$\hat{f} = \hat{f}(T, \hat{c}_1, \dots, \hat{c}_k, \lambda), \quad (18)$$

$$\tilde{f} = \gamma\sigma + \left( \tilde{\mu}_1 + \sum_{i=2}^k \tilde{\mu}_{i1} \tilde{c}_i \right), \quad (19)$$

$$\hat{f} = \tau\lambda + \left( \hat{\mu}_1 + \sum_{i=2}^k \hat{\mu}_{i1} \hat{c}_i \right). \quad (20)$$

Here, the excess free energy and the segregated amounts of components have been normalized by the total excess amounts  $\tilde{N} = \sum_i \tilde{N}_i$  and  $\hat{N} = \sum_i \hat{N}_i$ , respectively. Other notations include the normalized area  $\sigma = A/\tilde{N}$ , the normalized length  $\lambda = L/\hat{N}$ , and the low-dimensional analogs of the diffusion potentials:

$$\tilde{\mu}_{i1} = \frac{\partial \tilde{f}}{\partial \tilde{c}_i} - \frac{\partial \tilde{f}}{\partial \tilde{c}_1}, \quad (21)$$

$$\hat{\mu}_{i1} = \frac{\partial \hat{f}}{\partial \hat{c}_i} - \frac{\partial \hat{f}}{\partial \hat{c}_1}. \quad (22)$$



The excess concentrations  $\tilde{c}_i$  and  $\hat{c}_i$  can be put together in composition vectors  $\tilde{\mathbf{C}}$  and  $\hat{\mathbf{C}}$ , respectively.

Consider a  $k$ -dimensional space spanned by the molar free energies of the phases and the composition vectors (Fig. 1). The terms in parentheses in Eqs.(16), (19) and (20) define  $(k - 1)$ -dimensional hyperplanes, which we call  $\Lambda$ -planes because they originate from Legendre transformations of the free energy with respect to the concentrations. The  $\Lambda$ -planes are parallel to the tangential hyperplanes to the respective free energy functions  $f(\mathbf{C})$ ,  $\tilde{f}(\tilde{\mathbf{C}})$  and  $\hat{f}(\hat{\mathbf{C}})$  at fixed  $T$ ,  $\sigma$ , and  $\lambda$ . For a bulk phase, the  $\Lambda$ -plane coincides with the tangential hyperplane (assuming  $p = 0$ ). For a defect phase, the  $\Lambda$ -plane must be shifted by a positive amount of  $\gamma\sigma$  or  $\tau\lambda$  to touch the plot of the respective free energy function. In the initial state, when the phases are not in equilibrium with each other, their  $\Lambda$ -planes are generally not parallel. In the example shown in Fig. 1(a), the bulk phases  $\alpha$  and  $\beta$  are not in equilibrium with each other. If the free energy  $f_\beta(\mathbf{C})$  of phase  $\beta$  is above the  $\Lambda$ -plane of phase  $\alpha$ , then phase  $\beta$  is metastable relative to phase  $\alpha$ . In fact, phase  $\beta$  can be considered a defect in phase  $\alpha$ .

If the defect phases are in constrained equilibrium with each other and with the bulk phases, then all  $\Lambda$ -planes merge into a single hyperplane with linear coefficients equal to the diffusion potentials (Fig. 1(b)). The bulk phases are now in thermodynamic equilibrium with each other and their tangential planes merge into a common tangent plane. However, if the formation free energies  $\gamma$  and  $\tau$  of the defect phases remain positive, the defects are metastable relative to the bulk phases. They form equilibrium segregation atmospheres, but their existence costs the system extra free energy. When the system finally reaches its ground state, the formation free energies of the extended defects become zero. All  $\Lambda$  planes and all tangential planes merge into a common tangent plane to all phases (Fig. 1(c)).

It is instructive to consider in more detail the case of a single grain boundary in a binary solid solution, which is a  $(1@1@0)_2$  system with  $\pi = 2$ . Suppose the system is closed and the temperature and pressure are fixed ( $p = 0$ ). The molar free energy of the bulk phase, which we call phase  $\alpha$ , is a function of the solute concentration  $c_2$ . The bulk solution is initially in internal equilibrium. Next, we create a grain boundary in the system. Before it has a chance to equilibrate with the environment, it has the same chemical composition as the bulk phase (Fig. 2(a)); all excess properties are zero. Then we allow the boundary to equilibrate with the  $\alpha$  phase without changing the boundary area. This can be achieved by diffusion of the solute atoms. The boundary forms an equilibrium segregation atmosphere of the solute atoms. The process is accompanied by redistribution of the solute between the grain boundary and the bulk solution until a

constrained equilibrium is reached. If the segregation is positive ( $\tilde{c}_2 > 0$ ), the bulk solution is slightly depleted in the solute. The new chemical compositions of the boundary and the solution are such that the tangents to the respective free energy plots are parallel and the lever rule is satisfied for the given grain boundary area (Fig. 2(b)). The tangent line to the grain boundary free energy is a distance  $\gamma\sigma$  above that of the  $\alpha$  phase, indicating that the grain boundary phase is metastable. Finally, we allow the grain boundary to decrease its area to further reduce the total free energy. In the scenario shown in Fig. 2(c), the system reaches a ground state at a finite grain boundary area. The chemical compositions of the phases and the final grain boundary area are determined by the common tangent construction and the lever rule applied to the tie line  $a - b$ .

Fig. 3 presents an alternative scenario. In this case, the grain boundary again reaches a constrained equilibrium with the environment at a fixed area (Fig. 3(b)). As above, the new chemical compositions of the phases are dictated by the parallel tangent construction and the lever rule. The star symbol on the plot represents the total free energy of the system in this metastable state. If the grain boundary is allowed to vary its area, it will shrink and eventually disappear. The system will return to its initial single-phase state, in which the free energy is lower than in any state containing the grain boundary (Fig. 3(c)). This example demonstrates that full stabilization of a grain boundary is not always possible. It requires particular shapes of the free energy functions of both the grain boundary and the grains. Note that these shapes depend on temperature. A full grain boundary stabilization can be possible at one temperature but may become impossible at another temperature. In other words, a fully stabilized grain boundary can exist in a certain domain of the composition-temperature phase diagram of the bulk phase.

### 3 Fully stabilized defect structures

We next discuss possible morphologies of extended defects in a fully stabilized state. We focus on grain boundaries in a single-phase multicomponent solid solution as an example, although our conclusions are more general.

Grain boundary properties depend on five directional degrees of freedom in addition to internal variables, such as the local atomic density [31, 32]. Grain boundaries can also undergo structural [31, 33, 34] and segregation-induced [35] phase transformations. Partitioning into families of symmetry-related structures reduces the number of distinct grain boundary types. However, we still have an infinite number of boundaries that can potentially reach a full thermodynamic equilibrium. Meanwhile, the phase rule dictates that only a finite (usually small) number of grain boundary types can exist in the

thermodynamic ground state. How can nature reconcile the phase rule with the infinite pool of grain boundary types? Furthermore, the full equilibration is achieved for a specific grain boundary area and without triple junctions. What kind of geometric arrangements of grain boundaries can satisfy these requirements?

The answer depends on many factors, such as the crystallographic anisotropy of the boundary free energies, the temperature, and the free energy cost of small deviations from the strict  $\gamma = 0$  condition. At fixed temperature and pressure,  $\xi = k - 1$  grain boundaries can be equilibrated. Some possible morphologies are shown in Fig. 4. If  $\xi = 1$  and the  $\gamma = 0$  condition can be satisfied by a symmetrical tilt grain boundary, then the structure can be composed of lamellas with twin-related crystallographic orientations (Fig. 4(a)). The spacing  $l$  between the boundaries can be adjusted to match the equilibrium area. This structure contains no extended defects other than the grain boundaries and their intersections with the surface, which can be neglected for a sufficiently large sample size. The lamellas can also be organized into domains with orientations compatible with the crystal symmetry (Fig. 4(b)). The domain boundaries in this polysynthetic structure are additional extended defects, but their excess free energy can be neglected if they have a large (e.g., mesoscopic) size. For  $\xi > 1$ , the domains can be composed of periodic arrangements of lamellas with different crystallographic orientations ( $\leq \xi$ ) and widths adjusted to the required specific area. In this case, the grain boundaries need not be symmetric. Conventionally, lamella-based structures are vulnerable to capillary fluctuations and morphological instabilities (such as the Plateau-Rayleigh instability) unless the boundary free energy is highly anisotropic with deep cusps at the inclinations represented in the lamellas (Fig. 5(a)). But these instabilities would be suppressed for a fully stabilized grain boundary, for which the cusps in the  $\gamma$ -plot reach the origin of the plot, at which  $\gamma = 0$ , as shown schematically in Fig. 5(b).

An alternative morphology is a set of faceted grains embedded in a large matrix grain. When  $\xi = 1$ , the facets must have the same structure up to symmetry operations (Fig. 4(c)), while for  $\xi > 1$  the facets can be different and the grains can have more complex shapes (Fig. 4(d)). The grains do not have to be the same size. Like in the lamella case, strong crystallographic anisotropy is required to avoid morphological instabilities at elevated temperatures. The facet edges are additional extended defects with excess free energy. They can create a capillary pressure acting on the grains if  $\gamma > 0$ . However, their contribution to the total free energy can be negligible if the grains are sufficiently large. Also, when the system is in the ground state, the grain boundaries at special misorientations/inclinations have zero tension (Fig. 5(b)), and the force balance at the edges is of no concern.

At temperatures above the roughening transition, the excess free energy of grain boundaries becomes nearly isotropic. In this case, the uniform boundary model becomes a reasonable approximation, and all boundaries can be treated as one 2D phase. The embedded grains need not be faceted. If  $\gamma > 0$ , the embedded grain shape must be close to spherical. When  $\gamma \rightarrow 0$ , the capillary forces vanish and the grains have no particular shape or size. They may have a wide distribution of sizes and ameaba-like shapes (Fig. 4(e)). Another possible morphology is a maze crystal, which can be considered a particular case of the embedded-grain structure in which the embedded grain and the matrix form interpenetrating pathways. More generally, bi-continuous (Fig. 4(f)), tri-continuous (Fig. 4(g)), and similar interpenetrating morphologies are candidate ground-state structure when interfaces are nearly isotropic. They contain no triple junctions and can easily adjust the interface area per unit volume.

Yet another possible scenario that arises at high temperatures is that  $\gamma$  fluctuates around a zero value. The system will then reach a dynamic equilibrium between grain growth (when  $\gamma > 0$ ) and grain refinement (when  $\gamma < 0$ ) while maintaining a constant average boundary area. Such dynamic grain structures were observed in recent computer simulations [20]. In this case, the contribution of the configurational entropy to the free energy of the extended defects may no longer be negligible. Indeed, 1D defects could be analogous to polymer chains and 2D defects could be analogous to suspended graphene or lipid bilayers, all of which have configurational entropy contributions to free energy. After time-averaging over the fluctuations, the excess free energy may be zero.

The search for equilibrium microstructures that contain fully stabilized grain boundaries is a design problem that becomes especially interesting in the presence of interactions between the 1D/2D defects. So far, we have assumed that the defect excess free energies are simply additive, ignoring the interaction terms that depend on geometry. Dislocations have a long-range stress field  $\propto 1/r$ , and even fully relaxed grain boundaries have a stress field that decays exponentially with distance from the boundary plane. In finite-size polycrystals, (weak) interactions are unavoidable. For microstructures composed of isolated defects, such as those shown in Fig. 4(c,d,e), the design problem reduces to the optimization of a “superlattice” of 3D grains with a mesoscale lattice parameter  $l$ . With enough chemical complexity, it seems reasonable to expect that such a structure can reach a global minimum at an optimal value of  $l$ . This ground-state superlattice structure will resist grain coarsening or grain refinement, forming a “pseudo crystal” with internal interactions analogous to a ground-state atomic crystal. (Even though a ground-state atomic crystal has zero total stress, individual atomic pairs interact with attractive or repulsive interatomic forces, according to the Lennard-Jones interaction potential.)

As temperature or chemical composition change, this "pseudo crystal" structure can undergo reversible changes, assuming that the solute diffusion is fast enough to respond to the changes. The grain sizes and shapes can change, the lattice parameter  $l$  can increase ("thermal expansion") or decrease, and the superlattice itself can undergo sudden changes in the morphology and symmetry in a manner similar to structural phase transformations of the atomic crystal. At a high temperature, the superlattice can "melt" by transitioning to a spatially disordered arrangement of the grains.

## 4 Discussion and conclusions

Previous thermodynamic treatments of extended defects as low-dimensional phases considered only phase equilibria and phase transformations *within* a defect with a fixed area or length [27]. Thus, only constrained thermodynamic equilibria of the entire system were considered. The defects were in thermal, mechanical, and chemical equilibrium with their environment, but not in full equilibrium. The system containing extended defects was always in a metastable state. In this paper, we continued to treat extended defects as low-dimensional phases. However, we applied this treatment to address new questions not asked before, such as: Can a crystalline material with multiple extended defects reach a true thermodynamic equilibrium? If it can, what thermodynamic properties will the defect phases have? What kind of microstructure will the material have when it reaches the thermodynamic ground state?

To let the system reach the full thermodynamic equilibrium, we allowed the extended defects to vary their areas and lengths, which are the degrees of freedom that were previously frozen. In other words, the amounts of phases of *all* dimensionalities in a closed system were allowed to vary to reach full equilibrium. Two different scenarios were found. The defect phases can shrink in size and eventually disappear, leaving only bulk phases in the ground state. This happens if the defect formation free energies remain positive during the equilibration process. Grain growth in polycrystalline alloys is an example of this process. However, thermodynamics also permits a scenario in which some special extended defects remain. We have shown that the formation free energies of such defects in the ground state must be zero. In fact, such special "defects" are no longer defects but low-dimensional phases that can coexist thermodynamically with the conventional 3D phases. All driving forces for microstructure coarsening vanish, and the material becomes structurally stable. An example is offered by the hypothetical fully stabilized nanocrystalline alloys discussed in the literature [2–20]. However, many other types of stabilized materials, e.g., "pseudo crystals", can be imagined with unique properties in

the realms of ceramics or electronic materials. These structures with a finite characteristic lengthscale are forever immune to coarsening if the temperature and chemical composition are fixed. However, the said length scale can also vary when the intensive thermodynamic variables are changed, akin to thermal expansion or chemical expansion of atomic crystals.

In the beginning of the article, we mentioned intrinsic point defects whose free energy includes a configurational part due to their mobility and which are part of a bulk phase. However, many microstructures contain immobile point defects, such as dislocation nodes and quadruple points in polycrystalline materials. Such 0D defects (“defects in defects”) should be considered as 0D phases, and their degrees of freedom should be included in the phase rules. Considering that the fraction of atoms that reside in such phases is relatively small, we focused on 1D and 2D defects. Extension of our analysis to include 0D phases is straightforward.

An important outcome of this work is the realization that the stabilized extended defects must follow Gibbs’ phase rule generalized to phases of any dimensionality. This rule limits the number of defect types that the material can contain in the ground state. This number depends on the number of chemical components in the system and is in practice relatively small. The phase rule can serve as a guide for the design of thermodynamically stabilized materials. It also opens up an exciting new direction of searching for microstructures that contain a prescribed number of extended defects and are capable of adjusting the defect areas/length to satisfy the equilibrium conditions. We discussed several possible microstructures for a single-phase solid solution with grain boundaries. However, this simple case barely scratches the surface of the problem. Deeper and more systematic investigations are needed in the future.

Many other aspects of full stabilization call for future research. For example, solute diffusion is a critical factor that was not discussed here. During the equilibration process, the solute diffusion must be fast enough to sustain the segregation atmospheres at the defects and to maintain the low and eventually zero values of their formation energies. This is especially important for the dynamically equilibrated structures in which the defects constantly move and their free energies fluctuate between positive and negative values. Recent simulations suggest that slow solute diffusion can trap the structure in metastable states [19].

Another unexplored question is how the ground-state structures with defects would appear on phase diagrams. In the simple case of a binary solid solution (phase  $\alpha$ ) with a single grain boundary ((1@1@0)<sub>2</sub> system), the ground state structure can exist in a temperature-composition domain bounded by coexistence lines with other phases (Fig. 2(c)). At a fixed temperature, the ground states span the composition interval between the

end points  $a$  and  $b$  on the tie line. Near point  $a$ , the grain boundary area is infinitely small and phase  $\alpha$  is virtually a single crystal. Near point  $b$ , most atoms belong to the grain boundary while the grains are infinitely small. In reality, phase  $\alpha$  is likely to transform to another bulk phase before point  $b$  can be reached. Alternatively, the grain boundary can premelt when approaching point  $b$  and then fully melt at this point. In this scenario, the domain of the  $(1@1@0)_2$  system on the phase diagram is bounded by a solid-liquid coexistence field on the high-concentration side. In recent computer simulations [20], a stable polycrystalline state in a binary system was indeed observed under a solidus line on the phase diagram. Future research can show how general this trend is and what fully stabilized states can look like on the structural phase diagrams of more complex systems.

**Acknowledgement:** J. L. acknowledges support of the National Science Foundation, Division of Materials Research, under Award DMR-1923976. Y. M. was supported by the National Science Foundation, Division of Materials Research, under Award DMR-1708314.

## References

- [1] J. W. Gibbs, On the equilibrium of heterogeneous substances, in: The collected works of J. W. Gibbs, volume 1, Yale University Press, New Haven, 1948, pp. 55–349.
- [2] J. Weissmüller, Alloy thermodynamics in nano-structures, *J. Mater. Res.* 9 (1994) 4–7.
- [3] J. Weissmüller, Alloy effects in nanostructures, *Nanostructured Materials* 3 (1993) 261–272.
- [4] R. Kirchheim, Grain coarsening inhibited by solute segregation, *Acta Materialia* 50 (2002) 413–419.
- [5] F. Liu, R. Kirchheim, Nano-scale grain growth inhibited by reducing grain boundary energy through solute segregation, *Journal of Crystal Growth* 264 (2004) 385–391.
- [6] C. E. Krill, H. Ehrhardt, R. Birringer, Thermodynamic stabilization of nanocrystallinity, *International Journal of Materials Research* 96 (2005) 1134–1141.
- [7] L. S. Schvindlerman, G. Gottstein, Unexplored topics and potentials of grain boundary engineering, *Scripta Mater.* 54 (2006) 1041–1045.

- [8] R. Kirchheim, Reducing grain boundary, dislocation line and vacancy formation energies by solute segregation. I. Theoretical background, *Acta Mater.* 55 (2007) 5129–5138.
- [9] R. Kirchheim, Reducing grain boundary, dislocation line and vacancy formation energies by solute segregation. II. Experimental evidence and consequences, *Acta Mater.* 55 (2007) 5139–5148.
- [10] A. J. Detor, C. A. Schuh, Grain boundary segregation, chemical ordering and stability of nanocrystalline alloys: Atomistic computer simulations in the Ni-W system, *Acta Mater.* 55 (2007) 4221–4232.
- [11] J. R. Trelewicz, C. A. Schuh, Grain boundary segregation and thermodynamically stable binary nanocrystalline alloys, *Phys. Rev. B* 79 (2009) 094112.
- [12] T. Chookajorn, H. A. Murdoch, C. A. Schuh, Design of stable nano-crystalline alloys, *Science* 337 (2012) 951–953.
- [13] H. A. Murdoch, C. A. Schuh, Stability of binary nanocrystalline alloys against grain growth and phase separation, *Acta Mater.* 61 (2013) 2121–2132.
- [14] T. Chookajorn, C. A. Schuh, Thermodynamics of stable nanocrystalline alloys: A Monte Carlo analysis, *Phys. Rev. B* 89 (2014) 064102.
- [15] A. R. Kalidindi, C. A. Schuh, Stability criteria for nanocrystalline alloys, *Acta Mater.* 132 (2017) 128–137.
- [16] T. C. A. R. Kalidindi, C. A. Schuh, Nanocrystalline materials at equilibrium: A thermodynamic review, *JOM* 67 (2015) 2834–2843.
- [17] A. R. Kalidindi, C. A. Schuh, Stability criteria for nanocrystalline alloys, *J. Mater. Res.* 32 (2017) 1093–2002.
- [18] A. E. Perrin, C. A. Schuh, Stabilized nanocrystalline alloys: The intersection of grain boundary segregation with processing science, *Annual Review of Materials Research* 51 (2021) 241–268.
- [19] O. Hussein, Y. Mishin, A model of thermodynamic stabilization of nanocrystalline grain boundaries in alloy systems, *Acta Materialia* 281 (2024) 120404.
- [20] O. Hussein, Y. Mishin, A model of full thermodynamic stabilization of nanocrystalline alloys, 2025. Submitted to *Acta Materialia*. Preprint: arXiv:2503.17129.



- [21] C. C. Koch, R. O. Scattergood, K. A. Darling, J. E. Semones, Stabilization of nanocrystalline grain sizes by solute additions, *J. Mater. Sci.* 43 (2008) 7264–7272.
- [22] K. A. Darling, M. A. Tschopp, B. K. VanLeeuwen, M. A. Atwater, Z. K. Liu, Mitigating grain growth in binary nanocrystalline alloys through solute selection based on thermodynamic stability maps, *Comp. Mater. Sci.* 84 (2014) 255–266.
- [23] M. Saber, H. Kotan, C. C. Koch, R. O. Scattergood, Thermodynamic stabilization of nanocrystalline binary alloys, *J. Appl. Phys.* 113 (2013) 065515.
- [24] M. Saber, H. Kotan, C. C. Koch, R. O. Scattergood, A predictive model for thermodynamic stability of grain size in nanocrystalline ternary alloys, *J. Appl. Phys.* 114 (2013) 103510.
- [25] W. Xing, A. R. Kalidindi, D. Amram, C. A. Schuh, Solute interaction effects on grain boundary segregation in ternary alloys, *Acta Materialia* 161 (2018) 285–294.
- [26] N. Zhou, J. Luo, Developing thermodynamic stability diagrams for equilibrium-grain-size binary alloys, *Materials Letters* 115 (2014) 268–271.
- [27] T. Frolov, Y. Mishin, Phases, phase equilibria, and phase rules in low-dimensional systems, *J. Chem. Phys.* 143 (2015) 044706.
- [28] Y. Mishin, Thermodynamic theory of equilibrium fluctuations, *Annals of Physics* 363 (2015) 48–97.
- [29] J. W. Cahn, Thermodynamics of solid and fluid surfaces, in: W. C. Johnson, J. M. Blackely (Eds.), *Interface Segregation*, American Society of Metals, Metals Park, OH, 1979, pp. 3–23.
- [30] J. W. Gibbs, *The collected works of J. W. Gibbs*, volume 1, Yale University Press, New Haven, 1948.
- [31] T. Frolov, D. L. Olmsted, M. Asta, Y. Mishin, Structural phase transformations in metallic grain boundaries, *Nature Communications* 4 (2013) 1899.
- [32] J. Hickman, Y. Mishin, Extra variable in grain boundary description, *Phys. Rev. Materials* 1 (2017) 010601.
- [33] T. Frolov, Q. Zhu, T. Oppelstrup, J. Marian, R. E. Rudd, Structures and transitions in bcc tungsten grain boundaries and their role in the absorption of point defects, *Acta Mater.* 159 (2018) 123–134.

- [34] T. Meiners, T. Frolov, R. E. Rudd, G. Dehm, C. H. Liebscher, Observations of grain-boundary phase transformations in an elemental metal, *Nature* 579 (2020) 375–378.
- [35] T. Frolov, M. Asta, Y. Mishin, Segregation-induced phase transformations in grain boundaries, *Phys. Rev. B* 92 (2015) 020103(R).

## SUPPLEMENTARY INFORMATION

# The thermodynamic ground state of crystalline materials with defects

Ju Li and Yuri Mishin

In this Supplementary Information file, we show that the condition of zero formation free energies of all extended defects is equivalent to the condition of thermodynamic equilibrium among all 1D, 2D, and 3D phases present in the system. To simplify the derivation, we will assume that the phases have the same temperature at all times. In other words, we take for granted that the phases always remain in thermal equilibrium with each other.

A spatially uniform 3D phase composed of  $k$  chemical components is fully described by a single equation expressing its Helmholtz free energy as a function of temperature  $T$ , volume  $V$ , and the amounts  $N_i$  of the chemical components (measured in moles):

$$F = F(T, N_1, \dots, N_k, V). \quad (\text{S1})$$

Gibbs [30] referred to such equations as “fundamental” because they fully define all thermodynamic properties of the system.\* Such properties can be calculated by straightforward calculus without any additional information about the system.

The fundamental equation (S1) is a homogeneous function of first degree with respect to the extensive variables  $N_1, \dots, N_k$  and  $V$ . Applying the Euler theorem of homogeneous functions, we obtain

$$F = \sum_{i=1}^k \mu_i N_i - pV, \quad (\text{S2})$$

where  $\mu_i = \partial F / \partial N_i$  are the chemical potentials of the components and  $p = -\partial F / \partial V$  is pressure. On the other hand, taking the differential of Eq.(S1) we have

$$dF = -SdT + \sum_{i=1}^k \mu_i dN_i - pdV, \quad (\text{S3})$$

---

\*Gibbs used a more general fundamental equation in the form  $S = S(E, N_1, \dots, N_k, V)$ ,  $S$  being the system entropy and  $E$  the system energy. Since we assume thermal equilibrium across the system, we can conveniently reformulate the fundamental equation in terms of the free energy, as in Eq.(S1).

where  $S = -\partial F/\partial T$  is the system entropy.

Now consider an interface separating two phases or two grains within the same phase. It can be shown [27] that all interface properties are fully defined by the fundamental equation

$$\tilde{F} = \tilde{F}(T, \tilde{N}_1, \dots, \tilde{N}_k, A), \quad (\text{S4})$$

where  $A$  is the interface area,  $\tilde{F}$  is the excess free energy of the interface, and  $\tilde{N}_i$  are the excess amounts (in moles) of the chemical components. The excesses are defined using the dividing surface construction [30], in which the excess is taken relative to intensive properties of the homogeneous bulk phases extrapolated to the dividing surface.<sup>†</sup> Note that by deriving the interface thermodynamics starting from a fundamental equation, such as Eq.(S4), we treat interfaces as 2D phase. This interpretation is consistent with Gibbs [30], who treated all systems described by a fundamental equation the same way as he treated bulk phases.

Eq.(S4) has the same functional form as Eq.(S1) for bulk phases, except that the spatial dimensions of the interface are defined by its area  $A$  instead of the volume  $V$ . The excess free energy in Eq.(S4) is again a homogeneous function of first degree. Therefore, we can immediately rewrite the above equations in the interface variables:

$$\tilde{F} = \gamma A + \sum_{i=1}^k \tilde{\mu}_i \tilde{N}_i, \quad (\text{S5})$$

$$d\tilde{F} = -\tilde{S}dT + \gamma dA + \sum_{i=1}^k \tilde{\mu}_i d\tilde{N}_i, \quad (\text{S6})$$

where  $\tilde{S} = -\partial\tilde{F}/\partial T$  is the excess entropy. We denoted  $\tilde{\mu}_i \equiv \partial\tilde{F}/\partial\tilde{N}_i$  and defined

$$\gamma = \frac{\partial\tilde{F}}{\partial A} \quad (\text{S7})$$

as the interface free energy (interface tension).

Similarly, we can derive all thermodynamic properties of a 1D defect of length  $L$  from the fundamental equation

$$\hat{F} = \hat{F}(T, \hat{N}_1, \dots, \hat{N}_k, L), \quad (\text{S8})$$

which again implies that we treat the 1D defect as a phase. The excess free energy in Eq.(S8) is a homogeneous function of first degree similar to Eq.(S1) except for the

---

<sup>†</sup>Using the dividing surfaces simplifies thermodynamic derivations without loss of generality. All final results can be readily reformulated in terms of Cahn's generalized excess formalism [29] by mathematical rearrangements [27].

replacement of  $V$  by  $L$ . As above, we immediately write down the equations

$$\hat{F} = \tau L + \sum_{i=1}^k \hat{\mu}_i \hat{N}_i, \quad (\text{S9})$$

$$d\hat{F} = -\hat{S}dT + \tau dL + \sum_{i=1}^k \hat{\mu}_i d\hat{N}_i, \quad (\text{S10})$$

where  $\hat{S} = -\partial\hat{F}/\partial T$  is the excess entropy of the 1D defect. We denoted  $\hat{\mu}_i \equiv \partial\hat{F}/\partial\hat{N}_i$  and defined

$$\tau = \frac{\partial\hat{F}}{\partial L} \quad (\text{S11})$$

as the 1D defect free energy (line tension).

Next, we consider a compound system composed of  $\varphi_1$  1D defects,  $\varphi_2$  2D defects, and  $\varphi_3$  3D phases. Adding the above equations, we obtain the total free energy of the system,

$$\begin{aligned} F_{\text{tot}} &= \sum_{l=1}^{\varphi_1} \left( \tau_l L_l + \sum_{i=1}^k \hat{\mu}_i^{(l)} \hat{N}_i^{(l)} \right) \\ &+ \sum_{m=1}^{\varphi_2} \left( \gamma_m A_m + \sum_{i=1}^k \tilde{\mu}_i^{(m)} \tilde{N}_i^{(m)} \right) \\ &+ \sum_{n=1}^{\varphi_3} \left( -p_n V_n + \sum_{i=1}^k \mu_i^{(n)} N_i^{(n)} \right), \end{aligned} \quad (\text{S12})$$

and its differential

$$\begin{aligned} dF_{\text{tot}} &= \sum_{l=1}^{\varphi_1} \left( -\hat{S}_l dT + \tau_l dL_l + \sum_{i=1}^k \hat{\mu}_i^{(l)} d\hat{N}_i^{(l)} \right) \\ &+ \sum_{m=1}^{\varphi_2} \left( -\tilde{S}_m dT + \gamma_m dA_m + \sum_{i=1}^k \tilde{\mu}_i^{(m)} d\tilde{N}_i^{(m)} \right) \\ &+ \sum_{n=1}^{\varphi_3} \left( -S_n dT - p_n dV_n + \sum_{i=1}^k \mu_i^{(n)} dN_i^{(n)} \right). \end{aligned} \quad (\text{S13})$$

Suppose the system is closed (no matter exchange with the environment) and its volume and temperature are fixed. These constraints can be formulated by

$$\sum_{l=1}^{\varphi_1} d\hat{N}_i^{(l)} + \sum_{m=1}^{\varphi_2} d\tilde{N}_i^{(m)} + \sum_{n=1}^{\varphi_3} dN_i^{(n)} = 0, \quad i = 1, \dots, k, \quad (\text{S14})$$

$$\sum_{n=1}^{\varphi_3} dV_n = 0. \quad (\text{S15})$$

A system subject to these constraints spontaneously decreases  $F_{\text{tot}}$  until it reaches a global minimum in the equilibrium state. The necessary condition of the minimum is

$$\begin{aligned} (dF_{\text{tot}})_T &+ \sum_{i=1}^k \lambda_i \left( \sum_{l=1}^{\varphi_1} d\hat{N}_i^{(l)} + \sum_{m=1}^{\varphi_2} d\tilde{N}_i^{(m)} + \sum_{n=1}^{\varphi_3} dN_i^{(n)} \right) \\ &+ \omega \sum_{n=1}^{\varphi_3} dV_n = 0, \end{aligned} \quad (\text{S16})$$

where  $\lambda_i$  and  $\omega$  are Lagrange multipliers for the constraints (S14) and (S15), respectively. Inserting Eq.(S13) for  $dF_{\text{tot}}$ , the minimum condition becomes

$$\begin{aligned} &- \sum_{n=1}^{\varphi_3} (p_n - \omega) dV_n + \sum_{l=1}^{\varphi_1} \tau_l dL_l + \sum_{m=1}^{\varphi_2} \gamma_m dA_m \\ &+ \sum_{l=1}^{\varphi_1} \left( \sum_{i=1}^k \hat{\mu}_i^{(l)} + \lambda_i \right) d\hat{N}_i^{(l)} + \sum_{m=1}^{\varphi_2} \left( \sum_{i=1}^k \tilde{\mu}_i^{(m)} + \lambda_i \right) d\tilde{N}_i^{(m)} \\ &+ \sum_{n=1}^{\varphi_3} \left( \mu_i^{(n)} + \lambda_i \right) dN_i^{(n)} = 0, \end{aligned} \quad (\text{S17})$$

where all differentials are considered independent variations. When the minimum is reached, all differential coefficients vanish.

The mechanical equilibrium condition is obtained by setting the differential coefficients in front of the  $dV_n$  variations to zero, which gives

$$p_1 = p_2 = \dots = p_{\varphi_3}. \quad (\text{S18})$$

All bulk phases are at the same pressure.

The chemical equilibrium condition is obtained from the terms with the differentials of the amounts of chemical components, which gives

$$\mu_i^{(1)} = \mu_i^{(2)} = \dots = \mu_i^{(\varphi_3)} \equiv \mu_i, \quad i = 1, \dots, k, \quad (\text{S19})$$

$$\tilde{\mu}_i^{(1)} = \tilde{\mu}_i^{(2)} = \dots = \tilde{\mu}_i^{(\varphi_2)} = \mu_i, \quad i = 1, \dots, k, \quad (\text{S20})$$

$$\hat{\mu}_i^{(1)} = \hat{\mu}_i^{(2)} = \dots = \hat{\mu}_i^{(\varphi_1)} = \mu_i, \quad i = 1, \dots, k. \quad (\text{S21})$$

In other words, the chemical potential of every component is the same in all 1D, 2D, and 3D phases. All segregation atmospheres are in equilibrium with the surrounding bulk regions with respect to exchanges of chemical components.

Once the mechanical and chemical equilibrium conditions are satisfied, the free energy minimum condition (S17) reduces to

$$\sum_{l=1}^{\varphi_1} \tau_l dL_l + \sum_{m=1}^{\varphi_2} \gamma_m dA_m = 0. \quad (\text{S22})$$

At this point, the 3D phases are in equilibrium with each other, but the defect phases still remain in constrained equilibria. The full equilibration of the system requires that the total free energy be a minimum with respect to arbitrary variations of the lengths and areas of all extended defects. Such variations are represented by the differentials  $dL_l$  and  $dA_m$ . Thus the full equilibration requires that the defect free energies be zero:

$$\tau_1 = \tau_2 = \dots = \tau_{\varphi_1} = 0, \quad (\text{S23})$$

$$\gamma_1 = \gamma_2 = \dots = \gamma_{\varphi_2} = 0. \quad (\text{S24})$$

These are the conditions we sought to prove.

Returning to the case where the extended defects are in constrained but not full equilibrium, Eqs.(S9) and (S5) give the following equations for the excess free energies of the extended defects:

$$\hat{F}_l = \tau_l L_l + \sum_{i=1}^k \mu_i \hat{N}_i^{(l)}, \quad l = 1, \dots, \varphi_1, \quad (\text{S25})$$

$$\tilde{F}_m = \gamma_m A_m + \sum_{i=1}^k \mu_i \tilde{N}_i^{(m)}, \quad l = 1, \dots, \varphi_2. \quad (\text{S26})$$

Accordingly, the total free energy of a solid with metastable defects is

$$F_{\text{tot}} = \sum_{l=1}^{\varphi_1} \tau_l L_l + \sum_{m=1}^{\varphi_2} \gamma_m A_m + \sum_{i=1}^k \mu_i N_i - pV, \quad (\text{S27})$$

where  $N_i$  are the total amounts of the components in the system. In the thermodynamic ground state,

$$F_{\text{tot}} = \sum_{i=1}^k \mu_i N_i - pV. \quad (\text{S28})$$

The ground-state free energy follows the same equation as a single-phase solid.

It is now easy to derive the phase rule for an equilibrium multiphase system with extended defects. According to the fundamental equations (S1), (S4) and (S8), each phase is characterized by  $k + 1$  intensive parameters. The total number of intensive parameters

in all phases is  $(\varphi_1 + \varphi_2 + \varphi_3)(k + 1)$ . The three equilibrium conditions (S19), (S20) and (S21) plus the equality of temperatures in all phases impose

$$(k + 1) [\varphi_1 + \varphi_2 + \varphi_3 - 1] \tag{S29}$$

constraints. Eqs.(S18), (S23) and (S24) impose additional

$$\varphi_1 + \varphi_2 + (\varphi_3 - 1) \tag{S30}$$

constraints, bringing the total number of constraints to

$$(k + 2)(\varphi_1 + \varphi_2 + \varphi_3) - k - 2. \tag{S31}$$

The number of degrees of freedom of the system,  $\pi$ , is the number of intensive parameters minus the number of constraints, which gives

$$\pi = k + 2 - (\varphi_1 + \varphi_2 + \varphi_3). \tag{S32}$$

This is the generalized phase rule discussed in the main text.



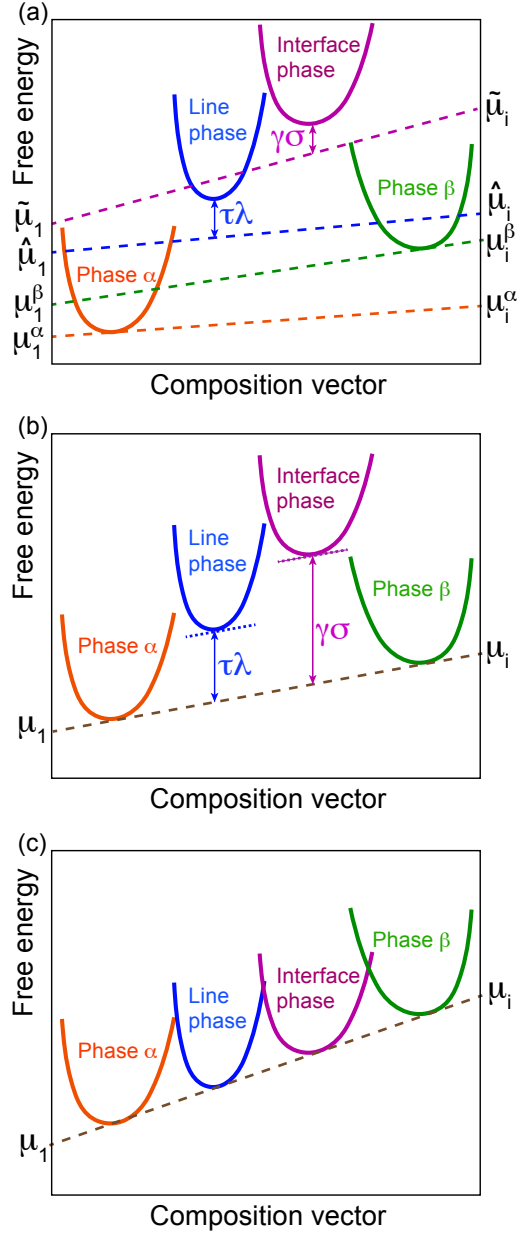


Figure 1: Conceptual diagrams illustrating the geometry of the defect phase thermodynamics. The molar free energy is plotted against the  $(k - 1)$ -dimensional composition vector. The multicomponent  $(2@1@1)_k$  alloy contains two bulk (3D) phases  $\alpha$  and  $\beta$ , a 1D defect phase (line defect), and a 2D defect phase (interface). (a) The phases are not in equilibrium with each other. (b) The system is in constrained equilibrium (the chemical potentials in all phases are equal). (c) The system is in thermodynamic ground state. The dashed lines represent the  $\Lambda$ -planes. The dotted lines in (b) represent tangential planes to the free energies of defect phases.

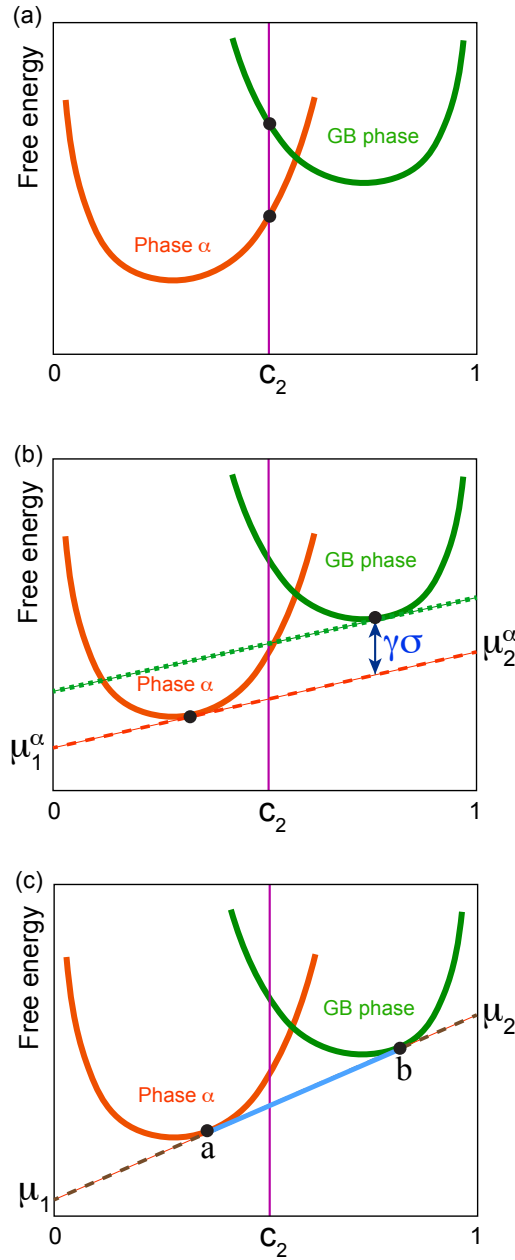


Figure 2: Free energy diagram of a binary solid solution  $\alpha$  containing a grain boundary labeled “GB phase”. The molar free energy is plotted against the solute concentration  $c_2$ . (a) Initial state after the boundary was inserted in the solution. (b) Grain boundary has been equilibrated with the  $\alpha$  phase without changing its area. (c) The grain boundary area has been adjusted to achieve thermodynamic equilibrium with the  $\alpha$  phase. The vertical line marks the fixed alloy composition. The dashed lines show the tangents to the phases. The black dots indicate the current states of the phases. The blue line  $a - b$  is a tie line between the two phases.

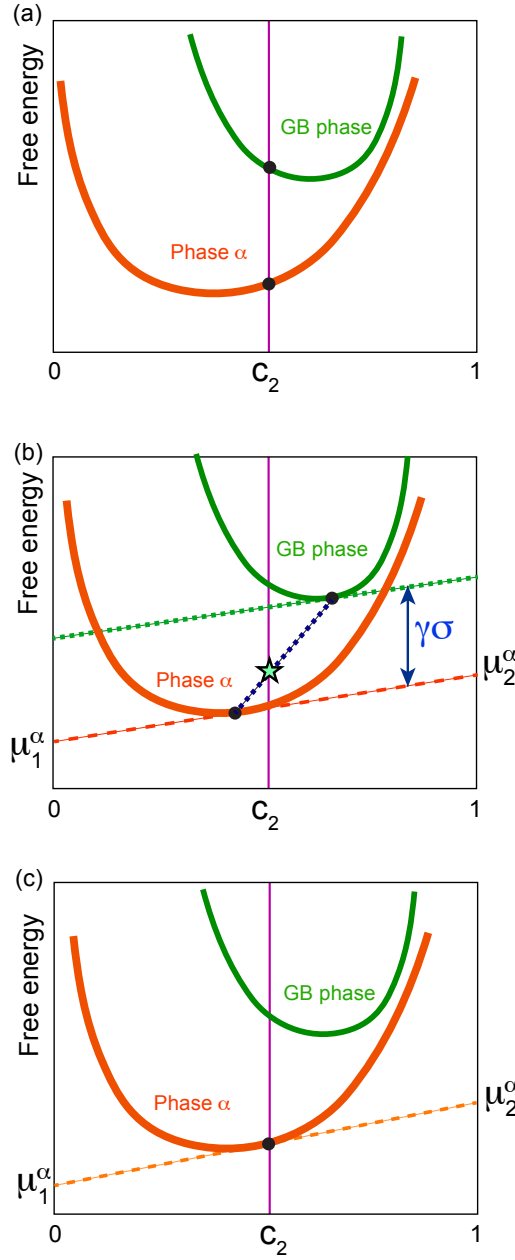


Figure 3: Free energy diagram of a binary solid solution  $\alpha$  containing a grain boundary (GB phase). The molar free energy is plotted against the solute concentration  $c_2$ . (a) Initial state after the boundary was inserted in the solution. (b) Grain boundary has been equilibrated with the  $\alpha$  phase without changing its area. (c) The grain boundary has disappeared to let the system reach the thermodynamic ground state. The vertical line marks the fixed alloy composition. The dashed lines show the tangents to the phases. The black dots indicate the current states of the phases. The dotted line in (b) is a tie line between the phases, and the star symbol marks the free energy of the system.

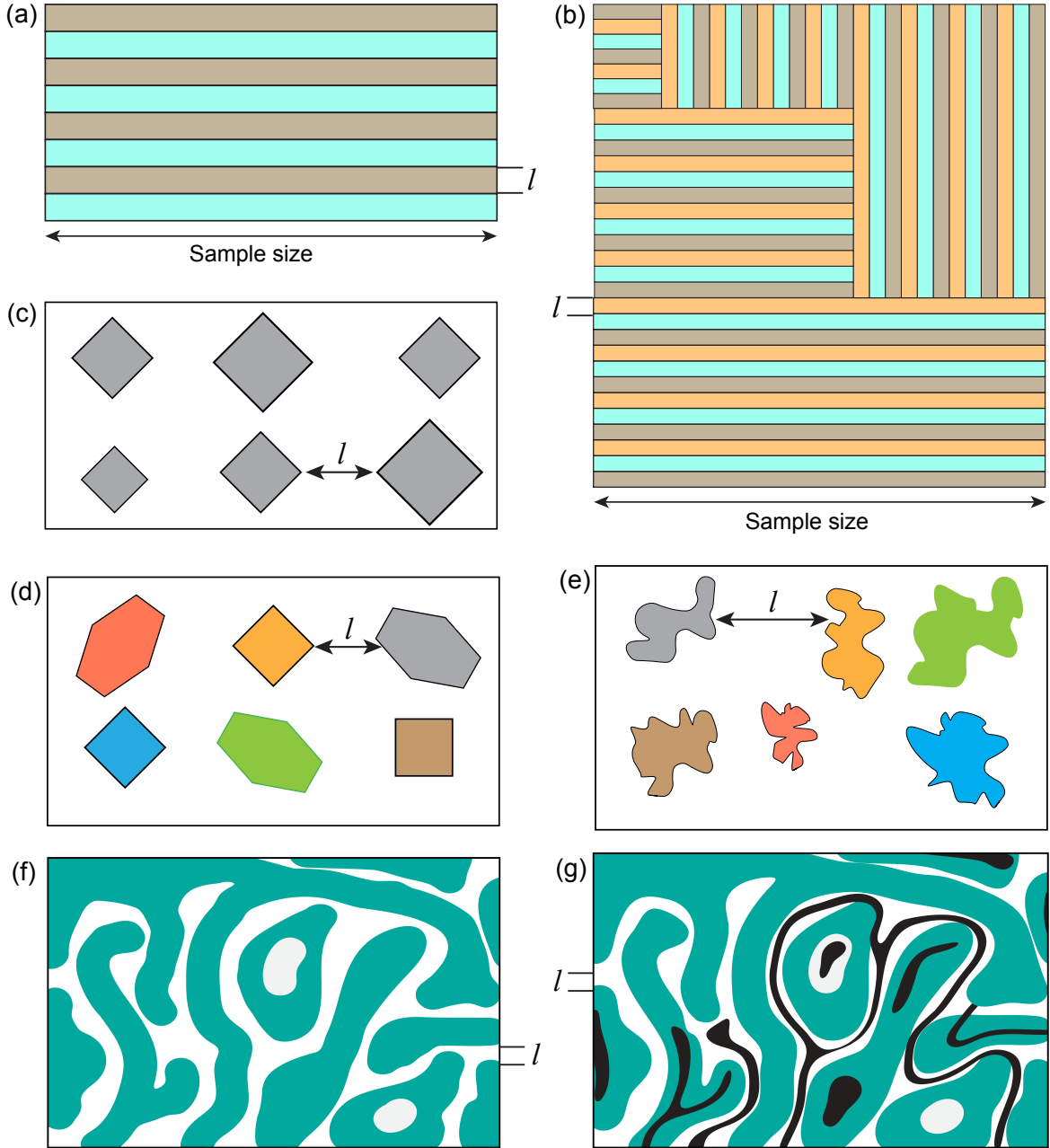


Figure 4: 2D schematics of possible ground state morphologies of a solid solution with grain boundaries ( $((1@1@0)_k)$  system). (a) Lamellar structure with symmetrical tilt grain boundaries. (b) Polysynthetic structure composed of lamellar domains. (c) Isolated grain arrangement for a single type of grain boundaries ( $\xi = 1$ ). (d) Isolated grain arrangement for several grain boundary types ( $\xi > 1$ ). (e) Isolated grains above the roughening transition. (f) Bi-continuous bicontinuous structure. (g) Tri-continuous tri-crystalline structure. The colors represent different lattice orientations. The characteristic distance  $l$  between the grains is indicated.

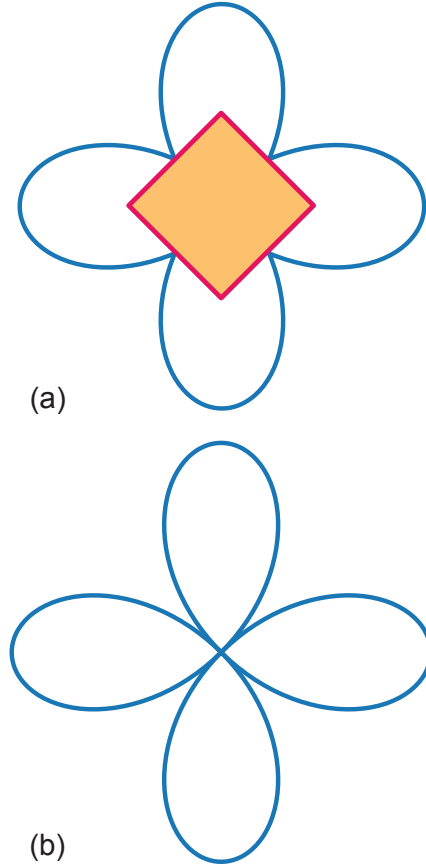


Figure 5: 2D schematic of possible  $\gamma$ -plots of a strongly anisotropic grain boundaries. (a) Grain boundary with  $\gamma > 0$ . The filled square shows the corresponding Wulff-Gibbs shape of an enclosed grain. (b) Grain boundary with  $\gamma = 0$ .